

# MULTIRESOLUTION GMRF MODELS FOR TEXTURE SEGMENTATION \*

Santhana Krishnamachari and Rama Chellappa

Department of Electrical Engineering  
Center for Automation Research and  
Institute for Advanced Computer Studies  
University of Maryland  
College Park, MD 20742

## ABSTRACT

A multiresolution model for Gauss Markov random fields (**GMRF**) is presented. Coarser resolution sample fields are obtained by either subsampling or local averaging the sample field at the fine resolution. Although Markovianity is lost under such resolution transformation, coarser resolution non-Markov random fields can be effectively approximated by Markov fields. We use a *local conditional distribution invariance approximation* to estimate the parameters of the coarser resolution processes from the fine resolution parameters. This multiresolution model is used to perform texture segmentation.

## 1. INTRODUCTION

Markov random field (**MRF**) models have been extensively used in image modeling to characterize prior beliefs about various image features such as textures, edges, region labels etc. and have been applied to restoration, segmentation and other image processing problems. One of the drawbacks of MRFs is that the associated optimization schemes are iterative and computationally expensive. Multiresolution schemes are one of the recourses to reduce the computational burden [6], [8], [4], [2]. Multiresolution schemes not only help to speed up the computation, but also bring together features that are widely separated in the fine resolution, resulting in their effective interaction at coarse resolutions. In this paper, we present a multiresolution GMRF model based on *local conditional distribution invariance* approximation and its application to texture segmentation problem.

Let  $\Omega^{(0)} = \{(i, j) : 0 \leq i \leq M - 1, 0 \leq j \leq M - 1\}$  be a lattice. Let  $X^{(0)}$  represent a random vector, obtained by ordering the random variables on the two-dimensional lattice  $\Omega^{(0)}$ , through a row-wise scan. The elements of  $\Omega^{(\cdot)}$  are indexed by  $s$ , where  $s = (s_1, s_2)$ . Let  $X^{(0)}$  be modeled by a GMRF, then

the joint probability density function of  $X^{(0)}$  can be written as follows:

$$P^{(0)}(X^{(0)} = x) = \frac{\exp\{-\frac{1}{2}x^T [\Sigma^{(0)}]^{-1} x\}}{(2\pi)^{\frac{M^2}{2}} (\det \Sigma^{(0)})^{\frac{1}{2}}} \quad (1)$$

where  $\Sigma^{(0)}$  is the covariance matrix of  $X^{(0)}$ .

Equivalently, the process  $X^{(0)}$  can be written in terms of a non-causal interpolative representation. For a site  $s$ , let  $\eta^{(0)}$  be the symmetric neighborhood, which contains the set of sites that are chosen to be the neighbors of  $X_s^{(0)}$ . In the rest of the paper, we always use  $r$  to index into the neighbor set.

$$X_s^{(0)} = \sum_{r \in \eta^{(0)}} \theta_r^{(0)} X_{s+r}^{(0)} + e_s^{(0)}$$

where  $e_s^{(0)}$ , is zero mean, spatially correlated, Gaussian noise with variance  $[\sigma^{(0)}]^2$ . Hence a GMRF process can be completely characterized by the set of parameters  $(\theta, \sigma^2)$ . Also  $X_s^{(0)}$  exhibits the Markov property,

$$\begin{aligned} P^{(0)}(X_s^{(0)} / X_t^{(0)}, \forall t \neq s, t \in \Omega^{(0)}) \\ = P^{(0)}(X_s^{(0)} / X_{s+r}^{(0)}, r \in \eta^{(0)}) \\ = \frac{1}{\sqrt{2\pi}[\sigma^{(0)}]^2} \exp\left\{-\frac{[x_s^{(0)} - \sum_{r \in \eta^{(0)}} \theta_r^{(0)} x_{s+r}^{(0)}]^2}{2[\sigma^{(0)}]^2}\right\} \end{aligned} \quad (2)$$

The power spectrum  $S_\omega^{(0)}$  of the process  $X^{(0)}$  can be shown to be:

$$S_\omega^{(0)} = \frac{[\sigma^{(0)}]^2}{1 - \sum_{r \in \eta^{(0)}} \theta_r^{(0)} \cos[\frac{2\pi}{M} r_1 \omega_1 + \frac{2\pi}{M} r_2 \omega_2]} \quad (3)$$

where  $\omega = \{\omega_1, \omega_2\}$ , and  $0 \leq \omega_1 \leq M - 1, 0 \leq \omega_2 \leq M - 1$ .

## 2. RESOLUTION TRANSFORMATION

Let  $\Omega^{(k)}$  represent the lattice obtained by subsampling (or subsampling followed by local averaging)

\* Appeared in Proc. of the ICASSP, pp 2407-2410, 1995.

$\Omega^{(0)}$ ,  $k$  times. In this paper we restrict ourselves to resampling transformation obtained by subsampling. But the results can be easily extended to block-to-point type transformation, where the coarse resolution data is obtained by averaging the fine resolution data over  $2 \times 2$  window.

The subsampling resolution transformation is defined as:

$$X_s^{(k)} = X_{2s}^{(k-1)}$$

defined for all  $s \in \Omega^{(k)}$ .

Equivalently,

$$X^{(k)} = D_0^k X_{(0)}$$

where the matrix  $D_0^k$ , has to be properly defined. The resulting subsampled process  $X^{(k)}$  is Gaussian, with covariance  $\Sigma^{(k)} = [D_0^k] \Sigma^{(0)} [D_0^k]^T$ .

The power spectrum of  $X^{(k)}$  can be shown to be [8]:

$$S_\omega^{(k)} = \frac{1}{2^{2k}} \sum_{r \in C_k} S_{\omega+r'}^{(0)} \quad (4)$$

where  $r' = (\frac{M}{2^k} r_1, \frac{M}{2^k} r_2)$  and  $C_k = \{r : 0 \leq r_1 \leq 2^k - 1, 0 \leq r_2 \leq 2^k - 1\}$ .

It can be observed that this is similar to aliasing due to sampling in time series applications. It can be observed that  $S_\omega^{(k)}$  cannot be written in the form of (3) with a finite neighborhood. Therefore, the subsampled process  $X^{(k)}$  is non-Markov, except for the special case of second order separable correlation processes [8].

### 3. MARKOV APPROXIMATION

In the case of GMRFs, it is possible to find the probability density function (pdf) of subsampled processes. However, if the lower resolution data are modeled by the exact non-Markov Gaussian measures, conventional optimization techniques based on Markov properties cannot be applied. In this section we show that it is possible to obtain very good Markov approximations for coarser resolution processes based on minimizing the Kullback-Leibler (KL) distance [7] between local conditional distributions.

Let  $P^{(k)}(X^{(k)})$  be the non-Markov pdf at the  $k$ th resolution then a GMRF approximation  $\hat{P}_g^{(k)}(X^{(k)})$  can be obtained such that, for  $r \in \eta^{(k)}$ , where  $\eta^{(k)}$  is the neighbor set,

$$\begin{aligned} \hat{P}_g^{(k)}(X_s^{(k)} / X_{s+r}^{(k)}) = \\ \arg \min_{P_g^{(k)}} D[P^{(k)}(X_s^{(k)} / X_{s+r}^{(k)}) \parallel P_g^{(k)}(X_s^{(k)} / X_{s+r}^{(k)})] \end{aligned} \quad (5)$$

where  $D(\cdot, \cdot)$  is the KL distance and  $P_g^{(k)}$  is the family of GMRF pdfs with the chosen neighborhood.

Since  $P_g^{(k)}$  belongs to the family of GMRF density,  $P_g^{(k)}(X_s / X_{s+r})$  will be of the form in (2). Following results can be obtained from (5).

The parameters  $(\hat{\theta}^{(k)}, [\hat{\sigma}^{(k)}]^2)$  corresponding to  $\hat{P}_g^{(k)}(X^{(k)})$  are obtained as follows:

$$\hat{\theta}^{(k)} = \arg \min_{\underline{\alpha}} E_{P^{(k)}} [X_s^{(k)} - \sum_{r \in \eta^{(k)}} \alpha_r X_{s+r}^{(k)}]^2 \quad (6)$$

and using the  $\hat{\theta}^{(k)}$  obtained, we can estimate the  $[\hat{\sigma}^{(k)}]^2$  as,

$$[\hat{\sigma}^{(k)}]^2 = E_{P^{(k)}} [X_s^{(k)} - \sum_{r \in \eta^{(k)}} \hat{\theta}_r^{(k)} X_{s+r}^{(k)}]^2.$$

To simplify the notations, let  $\mathbf{Y}$  be the vector containing the neighborhood random variables in a proper order. For a first order neighborhood,

$$\mathbf{Y} = \begin{pmatrix} X_{s+(1,0)}^{(k)} + X_{s-(1,0)}^{(k)} \\ X_{s+(0,1)}^{(k)} + X_{s-(0,1)}^{(k)} \end{pmatrix}$$

then,

$$\hat{\theta}^{(k)} = \arg \min_{\underline{\alpha}} E_p [X_s^{(k)} - \sum_{r \in \eta} \alpha_r Y_r]^2$$

$$[\hat{\theta}^{(k)}]^T = E_p (X_s^{(k)} \mathbf{Y}^T) [E_p (\mathbf{Y} \mathbf{Y}^T)]^{-1}$$

and,

$$\begin{aligned} [\hat{\sigma}^{(k)}]^2 &= E_p (X_s^{(k)2}) - E_p (X_s^{(k)} \mathbf{Y}^T) [E_p (\mathbf{Y} \mathbf{Y}^T)]^{-1} E_p (X_s^{(k)} \mathbf{Y}) \\ &= E_p (X_s^{(k)2}) - [\hat{\theta}^{(k)}]^T E_p (X_s^{(k)} \mathbf{Y}). \end{aligned}$$

If (6), results in a set of parameters that satisfies the stability (positivity) conditions (see [3]), then  $\hat{P}_g^{(k)}(X_s^{(k)} / X_{s+r}^{(k)})$  exactly equals  $P^{(k)}(X_s^{(k)} / X_{s+r}^{(k)})$ . This results in *local conditional distribution* invariance, which is a desirable property, especially because most of the optimization techniques such as simulated annealing [5], and iterated conditional mode [1] use the local conditional distribution. If positivity conditions are not satisfied, it is necessary to enforce the positivity constraints in the minimization of (6). Even though only conditional distribution invariance is emphasized in the above model, it can be shown that  $\hat{P}_g^{(k)}$  and  $P^{(k)}$  are "close" by comparing the corresponding power spectral densities.

The minimization requires the autocorrelation values  $E_{P^{(k)}}(X_s^{(k)} X_{s+r}^{(k)})$  which can be computed, given the GMRF parameters for  $X^{(0)}$  as shown below for subsampling resolution transformation.

$$\begin{aligned} X_s^{(k)} &= X_{2^k s}^{(0)} \\ E_{P^{(k)}}(X_s^{(k)} X_{s+r}^{(k)}) &= E_{P^{(0)}}(X_{2^k s}^{(0)} X_{2^k(s+r)}^{(0)}) \\ E_{P^{(0)}}(X_p^{(0)} X_q^{(0)}) &= \frac{1}{M^2} \sum_{s \in \Omega^{(0)}} \frac{(\lambda_{s_1}^{p_1} \lambda_{s_2}^{p_2})(\lambda_{s_1}^{q_1} \lambda_{s_2}^{q_2})}{1 - 2[\vartheta^{(0)}]^T \phi_s} \end{aligned}$$

where  $\lambda_i = \exp(\sqrt{-1} \frac{2\pi i}{M})$ .

#### 4. TEXTURE SEGMENTATION

Now, we present the application of the multiresolution model to texture segmentation. Texture segmentation problem is assigning a label, say from  $\{1, 2, \dots, V\}$  to the sites on the lattice, where the label stands for the texture class to which the site belongs to. Different textures in an image are modeled by GMRF models with different parameters represented by  $(\vartheta(v), \sigma^2(v))$ ,  $v \in \{1, 2, \dots, V\}$ . The intensity process given the label process is defined as follows:

$$\begin{aligned} P(X_s = x_s / L_s = v, X_r, L_r, r \in \eta) \\ = \frac{1}{\sqrt{2\pi\sigma^2(v)}} \exp\left\{-\frac{1}{2\sigma^2(v)} \left[x_s - \sum_{r \in \eta} \theta_r(v) x_{s+r}\right]^2\right\}. \end{aligned}$$

The label process is modeled by an MRF.

$$P(\underline{L} = l) = \frac{1}{Z} \exp\left\{\beta \sum_{s \in \Omega} U(l_s)\right\}$$

where,  $U(l_s)$  is the number of neighbors that have the same label as  $l_s$ .

Now given the intensity process, the label process can be estimated by minimizing a suitable criterion. The *maximum a posteriori* (MAP) error criterion solution can be obtained by:

$$\max_{\underline{L}} P(\underline{X}, \underline{L}) = \max_{\underline{L}} P(\underline{X}/\underline{L})P(\underline{L}). \quad (7)$$

This optimization requires stochastic relaxation methods and is computationally very expensive. So, we restrict ourselves to iterated conditional mode (ICM) method [1], a greedy algorithm that converges to a local maxima. The ICM solution is obtained by:

$$\begin{aligned} \max_{L_s} P(L_s/L_r, X_s, X_r) \\ = \max_{L_s} P(X_s/X_r, L_s, L_r)P(L_s/L_r) \\ = \min_{L_s} \log[\sigma(v)] - \beta U(L_s = v) \\ + \frac{1}{2\sigma^2(v)} \left[x_s - \sum_{r \in \eta} \theta_r(v) x_{s+r}\right]^2. \end{aligned} \quad (8)$$

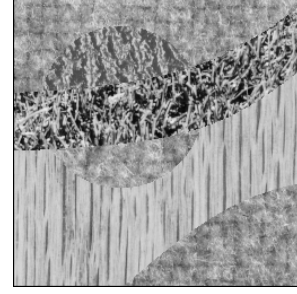


Figure 1:  
Brodatz Textures

First, it is assumed that the number of texture classes and the corresponding GMRF parameters at the fine resolution are known. Second, GMRF parameters at lower resolutions are obtained by the local conditional distribution invariance approximation as discussed before. Then segmentation is performed at the coarsest resolution by minimizing (8) with the corresponding parameters and the results of segmentation are passed on to the immediate higher resolution and so on until the fine resolution is reached. Figure 1 contains grass, calf leather, wool and wood textures. The original GMRF parameters at fine resolution are estimated by a maximum likelihood estimation. Figure 2 shows the single resolution segmentation with 14.27% misclassification and Figure 3 shows the multiresolution segmentation with 8.47% misclassification. Figure 4 shows a section of multispectral sensor image over Africa. (The image has been displayed after histogram equalization, the classes are not so disparate in the actual image). Unfortunately exact class maps are not available. However, we chose three classes corresponding to river, forest, deforestation. Figure 5 shows the single resolution result and Figure 6 shows the multiresolution result. Obviously, it can be observed that the multiresolution algorithm has performed better. We have experimented on simulated, Brodatz textures and real satellite images and have found the multiresolution scheme to perform better with much lesser computation. In general, this multiresolution GMRF model can be used in any application that uses GMRF models, like restoration, classification, segmentation.

#### ACKNOWLEDGEMENT

This research work was supported by the NSF Grant ASC 9318183.

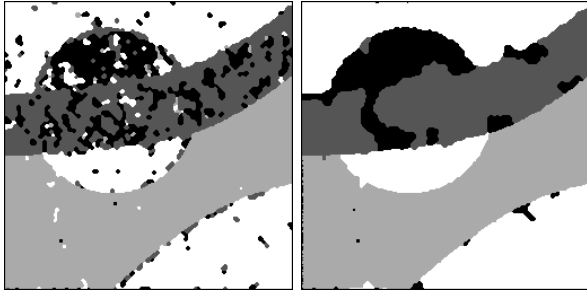


Figure 2:  
Single Resolution  
Segmentation

Figure 3:  
Multiresolution  
Segmentation

### REFERENCES

- [1] J. Besag, "Spatial Interaction and the Statistical Analysis of Lattice Systems," *Journal of the Royal Statistical Society*, Vol. 36, pp. 192–326, 1974.
- [2] C. Bouman and B. Liu, "Multiple Resolution Segmentation of Textured Images," *IEEE Trans. Patt. Anal. Mach. Intell.*, Vol. 13, pp. 99–113, Feb. 1991.
- [3] R. Chellappa, "Two-dimensional Discrete Gaussian Markov Random Field Models for Image Processing," in *Progress in Pattern Recognition* (L. N. Kanal and A. Rosenfeld, eds.), pp. 79–112, Elsevier, 1985.
- [4] F. S. Cohen and D. B. Cooper, "Simple Parallel Hierarchical and Relaxation Algorithms for Segmenting Noncausal Markovian Random Fields," *IEEE Trans. Patt. Anal. Mach. Intell.*, Vol. 9, pp. 195–219, March 1987.
- [5] S. Geman and D. Geman, "Stochastic Relaxation, Gibbs Distribution and the Bayesian Restoration of Images," *IEEE Trans. Patt. Anal. Mach. Intell.*, Vol. 6, pp. 721–741, Nov 1984.
- [6] B. Gidas, "A Renormalization Group Approach to Image Processing," *IEEE Trans. Patt. Anal. Mach. Intell.*, Vol. 11, No. 2, pp. 164–180, 1989.
- [7] S. Kullback and R. A. Leibler, "On Information and Sufficiency," *Ann. Math. Stat.*, Vol. 22, pp. 79–86, 1951.
- [8] S. Lakshmanan and H. Derin, "Gaussian Markov Random Fields at Multiple Resolutions," in *Markov Random Fields: Theory and Applications* (R. Chellappa, ed.), pp. 131–157, Academic Press, 1993.



Figure 4: Remote Sensed Image

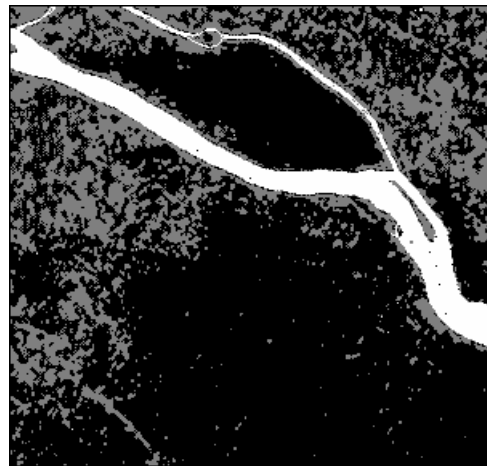


Figure 5: Single Resolution Segmentation

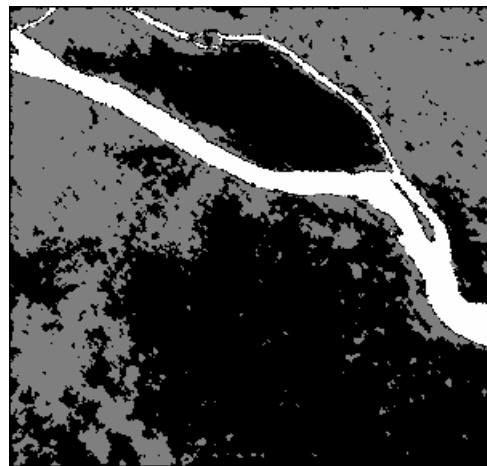


Figure 6: Multiresolution Segmentation